

Magnetic rogue wave in a perpendicular anisotropic ferromagnetic nanowire with spin-transfer torque

Fei Zhao¹, Zai-Dong Li^{1,*} and Qiu-Yan Li¹, Lin Wen², Guangsheng Fu¹, W. M. Liu²

¹*Department of Applied Physics and School of Information Engineering,
Hebei University of Technology, Tianjin 300401, China and*

²*Beijing National Laboratory for Condensed Matter Physics,
Institute of Physics, Chinese Academy of Sciences, Beijing 100080, China*

We present the current controlled motion of dynamic soliton embedded in spin wave background in ferromagnetic nanowire. With the stronger breather character we get the novel magnetic rogue wave and clarify its formation mechanism. The generation of magnetic rogue wave is mainly arose from the accumulation of energy and magnons toward to its central part. We also observe that the spin-polarized current can control the exchange rate of magnons between envelope soliton and background, and the critical current condition is obtained analytically. Even more interesting is that the spin-transfer torque plays the completely opposite role for the cases of below and above the critical value.

PACS numbers: 75.78.-n, 75.40.Gb, 72.25.Ba

I. INTRODUCTION

In ferromagnet nanowires, the deviation of magnetization from the ground state results in the excitation of spin waves. Their attractive interaction and instabilities contribute to the existence of topological and dynamic solitons. The dynamics of magnetization in a soliton can be well described by the famous Landau-Lifshitz-Gilbert equation [1].

The topological soliton, now namely domain wall (DW), connecting two vacua describes an inhomogeneous state of magnetization and it cannot be reduced to the ground state by any finite deformation [2]. So it has technological application in race track memory [3]. The field-driven DW motion has been studied extensively in thin films [4] and recently in magnetic nanowires [5–10]. These studies show that the DW travelling speed in magnetic materials conventionally depends on the strength of a constant magnetic field as the external field is below the Walker-breakdown value [11, 12]. Above this critical value, the DW develops a variational complex internal structure which results in temporal oscillation of DW velocity [5, 6, 13, 14]. Recently, many studies demonstrate that the spin-polarized current can cause many unique phenomena for magnetization motion, which attributes to spin-transfer effect [15]. With this consideration the modified Landau-Lifshitz-Gilbert equation [16–18] including spin-transfer torque has been derived to describe such current-induced magnetization dynamics. With the remarkable experimental successes measuring the motion of a DW, considerable progresses have been made to understand the current-induced DW motion in magnetic nanowires [17–23]. This current induced magnetization motion possesses of different character from that driven by an magnetic field, and the spin-transfer

torque can induce not only precession but also damping role for the motion of magnetization.

On the other hand, the dynamic soliton describes the localized states of magnetization which can be reduced to a uniform magnetization by continuous deformation, so that the excited ferromagnet makes a transition to the ground state. Therefore, a dynamic soliton is sometimes said to be topologically equivalent to the ground state. Also, the motion of dynamic soliton is of topic research in confined ferromagnetic materials [24–27], especially with the generation and detection of magnons excitation [28] in a magnetic multilayer. Driven by the adiabatic spin-transfer torque, the dynamic soliton solutions for isotropic case [29] and uniaxial anisotropic case [30] are investigated carefully, where the corresponding solutions show the characteristic breather behavior for magnetization motion in ferromagnetic nanowire. However, the current driven motion of the dynamic soliton are not well explored carefully.

In this paper, we present the generation of a novel *magnetic rogue wave* solution under stronger breather characters in a perpendicular anisotropic ferromagnetic nanowire driven by spin-transfer torque, which is similar to optical rogue wave in fiber [31, 32]. The formation mechanism of magnetic rogue wave is clarified carefully. In this process, we observe that the spin-polarized current can control the magnons exchange rate between the envelope soliton and background, and the critical current condition is obtained analytically. Moreover, the spin-transfer torque play the completely opposite role for the cases of below and above the critical value.

II. CURRENT DRIVEN INTERACTION OF SPIN WAVE AND A DYNAMIC SOLITON IN FERROMAGNETIC NANOWIRE

When a spin-polarized electric current flows the ferromagnetic nanowire, the localized magnetization dynam-

*Corresponding author, E-mail: zdli2003@yahoo.com

ics can be described by the modified Landau-Lifshitz equation [17, 18] with the spin-transfer torque,

$$\frac{\partial \mathbf{M}}{\partial t} = -\gamma \mathbf{M} \times \mathbf{H}_{\text{eff}} + \frac{\alpha}{M_s} \mathbf{M} \times \frac{\partial \mathbf{M}}{\partial t} + \tau_s, \quad (1)$$

where γ is the gyromagnetic ratio, α is the Gilbert damping parameter, and \mathbf{H}_{eff} represents the effective magnetic field including the exchange field, the anisotropy field and the external field. For a perpendicular anisotropic ferromagnetic nanowire, the effective magnetic field takes the form $\mathbf{H}_{\text{eff}} = (2F/M_s^2) \partial^2 \mathbf{M} / \partial x^2 + [(H_K/M_s - 4\pi) M_z + H_{\text{ext}}] \mathbf{e}_z$, where F is the exchange constant, H_K denotes the energetic anisotropy coefficient, H_{ext} is the applied external magnetic field, and \mathbf{e}_z is the unit vector along the z -axis. The last term τ_s in Eq. (1) denotes the spin-transfer torque, which describes the injected current can be polarized and produces a torque acting on the local magnetization. This adiabatic spin-transfer torque is of the form $\tau_s = b_J (\partial \mathbf{M} / \partial x)$ [18], where $b_J = P j_e \mu_B / (e M_s)$, P is the spin polarization of the current, j_e is the electric current density and flows along the x direction, μ_B is the Bohr magneton, e is the magnitude of electron charge.

Introducing the normalized magnetization, i.e., $\mathbf{m} = \mathbf{M} / M_s$, we can simplify Eq. (1) as the dimensionless form

$$\frac{\partial \mathbf{m}}{\partial t} = -\mathbf{m} \times \mathbf{h}_{\text{eff}} + \alpha \mathbf{m} \times \frac{\partial \mathbf{m}}{\partial t} + A_J \frac{\partial \mathbf{m}}{\partial x}, \quad (2)$$

where $\mathbf{h}_{\text{eff}} = \mathbf{H}_{\text{eff}} / M_s$ and $A_J = b_J t_0 / l_0$. The time t and space coordinate x have been rescaled by the characteristic time $t_0 = 1 / [\gamma (H_K - 4\pi M_s)]$ and length $l_0 = \sqrt{2F / [(H_K - 4\pi M_s) M_s]}$, respectively. As discussed in our pervious work [30], Eq. (2) admits the excited states, i.e., spin wave and a dynamic soliton. For the perpendicular anisotropic ferromagnetic nanowire, these two types of excited state denote the small deviation of magnetization from the ground state. Therefore, a reasonable complex function q can be introduced to replace the components of normalized magnetization [2], i.e., $q \equiv m_x + i m_y$ and $m_z^2 = 1 - |q|^2$. Under the long-wavelength approximation [2] and without damping, Eq. (2) becomes the integrable nonlinear Schrödinger equation

$$i \frac{\partial q}{\partial t} = \frac{\partial^2 q}{\partial x^2} + \frac{1}{2} q |q|^2 + i A_J \frac{\partial q}{\partial x} - \omega_0 q, \quad (3)$$

where $\omega_0 = 1 + H_{\text{ext}} / (H_K - 4\pi M_s)$.

It is easy to find two basic solutions of Eq. (3). One is $q = 0$, which corresponds to the ground state $\mathbf{m} = (0, 0, 1)$. The other solution is spin wave, i.e., $q = A_c e^{-i(k_c x - \omega_c t)}$ with ω_c and k_c being the dimensionless frequency and wave number, respectively. In perpendicular anisotropic ferromagnetic nanowire, the interaction of spin waves is attractive and their instabilities lead to macroscopic phenomena, i.e., the appearance of a spatially localized magnetic excited state (topological or dynamic soliton). As shown later, the interaction of spin wave and a dynamic soliton can result in the *novel*

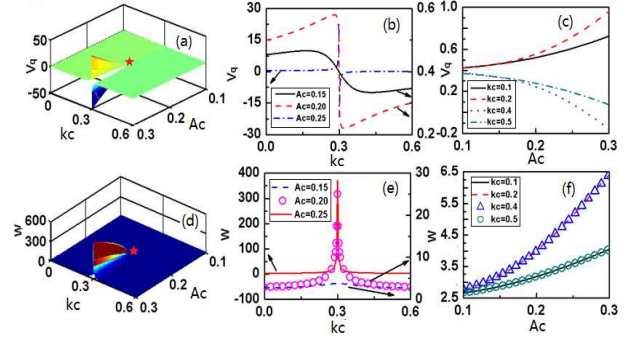


FIG. 1: (Color online) Breather velocity V_q and width W vs the amplitude A_c and wave number k_c of spin wave. The other parameters are $u_1 = 0.2$, $\nu_1 = -0.3$ and $A_J = 0.2$. (a) and (d): The soliton velocity V_q and width W vs with A_c and k_c . The red star signs the location of the rogue wave. (b) and (c) The dependence of velocity on A_c and k_c . (e) and (f) The dependence of velocity on A_c and k_c .

magnetic rogue wave which can be realized by adjusting the relation of wave number and amplitude for spin wave and a dynamic soliton. To this purpose, one should get the solution on the spin wave background.

By employing Darboux transformation [30, 33] and performing a tedious calculation, we obtain such solution

$$q = e^{i\varphi} [A_c + 2u_1 (\Delta_1 + i\Delta_2) / \Delta], \quad (4)$$

where $\varphi = \omega_c t - k_c x$, $\Delta = \cosh \theta + a \cos \beta$, $\Delta_1 = a \cosh \theta + \cos \beta$, $\Delta_2 = b \sinh \theta + c \sin \beta$, here $\theta = D_R x + (D\delta)_R t + x_0$, $\beta = D_I x + (D\delta)_I t - t_0$, $a = 2A_c L_R / (|L|^2 + A_c^2)$, $b = 2A_c L_I / (|L|^2 + A_c^2)$, $c = (|L|^2 - A_c^2) / (|L|^2 + A_c^2)$, and the subscript R and I represent the real and imaginary part, respectively. The other parameters are $L = -ik_c - D - \lambda$, $D = [(ik_c + \lambda)^2 - A_c^2]^{1/2}$, and $\delta = -i\lambda - k_c + A_J$, where $\lambda = u_1 + i\nu_1$. Here x_0 , t_0 , A_c , k_c , u_1 , and ν_1 are the real constants, and without loss of generality we assume that A_c and u_1 are non-negative real constants.

The solution in Eq. (4) exhibits a dynamic soliton solution embedded in spin wave background. Two types of excited states (spin wave and a dynamic soliton) can be recovered from Eq. (4): a) As the spin wave amplitude and wave number vanishes, namely $A_c = k_c = 0$, we can get a dynamic soliton, $q_1 = 2u_1 e^{i(\beta_1 + \omega_c t)} / \cosh \theta_1$, with $\theta_1 = u_1 x + u_1 (2\nu_1 + A_J) t + x_0$ and $\beta_1 = \nu_1 x - (u_1^2 - \nu_1^2 - A_J \nu_1) t - t_0$. This solution corresponds to the dynamic precession of magnetic soliton on the ground state background, where the soliton moves with the velocity $v = -2\nu_1 - A_J$, and the components m_x and m_y precess around m_z with the amplitude $A_q = 2u_1 / \cosh \theta_1$ and the frequency $\omega_q = u_1^2 - \nu_1^2 - A_J \nu_1 + \omega_c$. It clearly demonstrates that the spin current term A_J can change the dynamic soliton velocity and the precessional frequency. In addition, the solution q_1 represents in fact the static magnetic soliton with three integrals of the motion and the uniform magnon density $|q_1|^2 = 2u_1$ along the direction of soliton propagation. b) When the amplitude

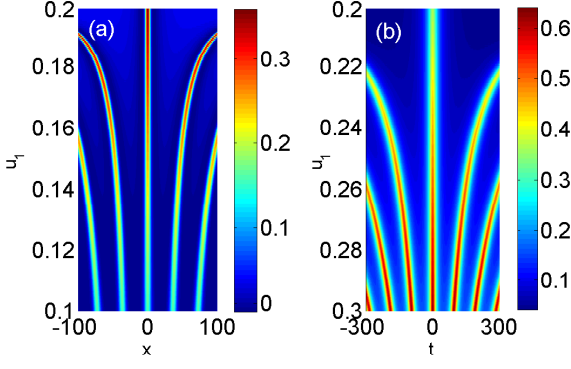


FIG. 2: (Color online) The evolution of magnetic soliton in the limit processes $u_1 \rightarrow A_c^-$ (a) and $u_1 \rightarrow A_c^+$ (b). Other parameters are $A_c = 0.2$, $A_J = 0.2$, $k_c = -\nu_1 = 0.003$, and $x_0 = t_0 = 0$.

of dynamic soliton vanishes, namely $u_1 = 0$, Eq. (4) reduces to spin wave solution $q = A_c e^{-i(k_c x - \omega_c t)}$, in which the magnon density is also constant.

From Eq. (4), we observe that the solution commonly exhibits a breather character and a time periodic modulation for soliton amplitude, which in fact denotes the interaction between the localized process of spin wave background and the periodization process of magnetic soliton. The properties of the soliton solution are characterized by the slope direction $V_\theta \equiv D_R x + (D\delta)_{Rt}$, the breather propagation velocity $v_q \equiv -(D\delta)_R/D_R$ and the soliton width $1/D_R$. With the expressions of D and δ , we find that the soliton velocity and width are modulated by the amplitude A_c and wave number k_c of spin wave as shown in Fig. 1(a) and 1(d). The absolute value of soliton velocity and soliton width increases with increasing A_c as shown in Fig. 1(c) and 1(f). Moreover, as the modulation parameter A_c increases continuously, the soliton velocity will be affected mainly by the value of k_c near $-\nu_1$. When $k_c = -\nu_1$, the soliton velocity and width is maximal, respectively, as shown in Fig. 1(b) and 1(e). This phenomena in fact ascribes to magnonic spin-transfer torque [34] which denotes the transfer of spin angular momentum from spin wave background to a dynamic soliton, and it will be discussed elsewhere in detail. On the basis of Eq. (4), as the modulation parameter u_1 approaches A_c , some novel properties will be presented. Magnetic rogue wave solution will be excited in ferromagnetic nanowire which leads to some fantastic phenomena.

III. NOVEL MAGNETIC ROGUE WAVE

In terms of our previous discussion [30] for the solution in Eq. (4), we have known that the critical point $u_1 = A_c$ forms a dividing line between the modulation instability process ($u_1 > A_c$) and the periodization process ($u_1 < A_c$) under the condition $\nu_1 = -k_c$. It leads

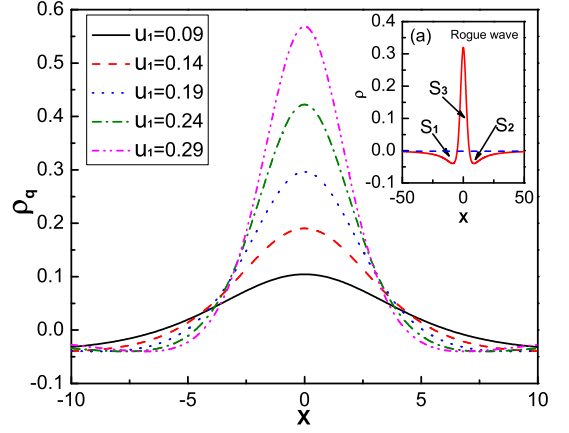


FIG. 3: (Color online) The magnon density distribution against the background for the different parameter u_1 , which ranges from 0.09 to 0.29 in 0.05 steps. (a) The magnon density distribution against the background for the excited formation of magnetic rogue wave. Other parameters are $A_c = 0.2$, $A_J = k_c = 0.1$ and $x_0 = t_0 = 0$.

to the different physical behavior how the breather character depends strongly on the modulation parameter u_1 as shown in Fig. 2. Fig. 2 shows two different asymptotic behavior in the limit processes $u_1 \rightarrow A_c^-$ (and A_c^+) under the condition $\nu_1 = -k_c$, respectively. The former demonstrates a spatial periodic process of a soliton and we observe that the spatial separation of adjacent peak and each peak value increases rapidly as the modulation parameter u_1 approaching A_c , respectively. The latter shows a localized process of the spin-wave background along the slope direction $K_\beta = -(D\delta)_I/D_I$ for $t_0 = 0$. In this case, the temporal separation of adjacent peak also increases rapidly as the modulation parameter u_1 approaching A_c , while each peak value takes the rapid decrease. Even more interesting, in the limit case of $u_1 \rightarrow A_c$, i.e., the pentagram sign indicated in Fig 1(a) and (d), we get the *novel magnetic rogue wave*

$$Q_1 = A_c e^{i\varphi} \left[\frac{4(1 - itA_c^2)}{t^2 A_c^2 \eta + 2txA_c^2 \zeta + \varepsilon} - 1 \right], \quad (5)$$

where $\eta = A_J^2 + A_c^2 + 4k_c^2 - 4A_J k_c$, $\zeta = A_J - 2k_c$, and $\varepsilon = 1 + x^2 A_c^2$. Eq. (5) shows the typical rogue wave feature that the magnons accumulated from spin wave background converge a single hump with the critical amplitude $A_Q = 3A_c$. It implies that the localization wave is captured completely at $x = 0$ and $t = 0$ by spin wave background. As shown in Fig. 3, the realization of magnetic rogue wave in Eq. (5) attributes to that the aggregation of magnons gradually increases as u_1 approaches A_c^- , while decreases gradually with u_1 approaches A_c^+ . The temporal localization magnetic rogue wave is excited as $u_1 \rightarrow A_c$ with the magnon density peak $|q|^2 = 9A_c^2$.

In order to investigate deeply the properties of magnetic rogue wave in ferromagnetic nanowire, the analysis

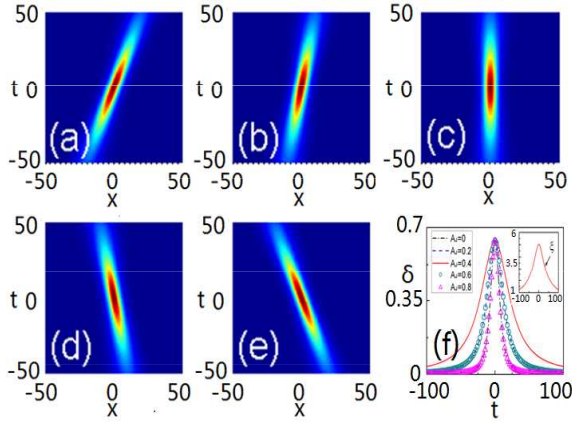


FIG. 4: (Color online) (a)-(e) The formation region in space (x, t) for magnetic rogue wave with different current. The parameter A_J ranges from 0 to 0.8 in 0.2 steps. (f) The nonuniform exchange of magnons between rogue wave and background for the different spin current. The inset figure in (f) denotes the maximal accumulation (or dissipation) process for the critical current value $A_J = 2k_c$. Other parameters are $A_c = 0.2$ and $k_c = 0.2$.

for the magnon density distribution against the background plays a major role, which is defined by the quantity $\rho_q(x, t) = |q_1(x, t)|^2 - |q_1(x = \pm\infty, t)|^2$. In Fig. 3 we plot the evolution of magnon density distribution for the breather solution in Eq. (4), which ultimately demonstrates the formative mechanism of magnetic rogue wave solution in ferromagnetic nanowire. With the modulation parameter u_1 approaches A_c , the magnons in the background gradually gather toward to each individual central part and the envelope becomes sharper. Specially, as shown the inset (a), the critical peak will appear under the condition $u_1 \rightarrow A_c$, i.e., the magnetic rogue wave is excited.

With Eq. (5) and the quantity $\rho = |Q_1(x, t)|^2 - |Q_1(x = \pm\infty, t)|^2$ we obtain the magnon density distribution in a magnetic rogue wave

$$\rho = 8A_c^2 \frac{\Gamma_1 - \Gamma_2}{(\Gamma_1 + \Gamma_2)^2}, \quad (6)$$

where $\Gamma_1 = 1 + t^2 A_c^4$, $\Gamma_2 = A_c^2 (x + t(A_J - 2k_c))^2$, and Eq. (6) implies the integral $\int_{-\infty}^{+\infty} \rho(x, t) dx = 0$ for arbitrary time. From the condition $\rho_Q(\pm 1/A_c, 0) = 0$, we can define the spatial width of the hump part in rogue wave as $2/A_c$. A detail calculation shows that at a fixed time the loss of magnons in background completely transfer to hump, i.e., the area relation $\mathbf{S}_1 + \mathbf{S}_2 = \mathbf{S}_3$. These results clearly illustrate that the generation of magnetic rogue wave with stronger breather character is mainly arose from the gathering energy and magnons from the background toward to its central part, and the loss of magnons in background completely transfer to the hump part in magnetic rogue wave.

The other interesting fundamental problem is that how rogue wave gather magnons and energy toward to

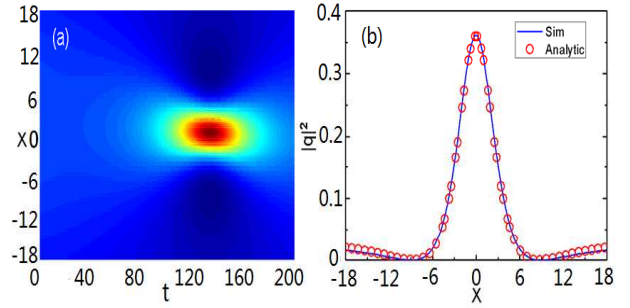


FIG. 5: (Color online) (a) Evolution of the numerical magnetic rogue wave. (b) Comparison of magnon density between the numerical solution (in solid curve) and ideal solution (in 'o'). Other parameter are $A_c = 0.2$, $u_1 = 0.19$, $x_0 = 0.72$, $A_J = 0.01$, $k_c = 0.2$ and $\omega = 0.2$.

its central part from the background. This can be explained by the quantity $\delta(x, t) \equiv \lim_{l_Q \rightarrow \pm\infty} |Q_1(x, t) - Q_1(x = l_Q, t)|^2$. With Eq. (5) we obtain

$$\delta(x, t) = 16A_c^2 \frac{\Gamma_1}{(\Gamma_1 + \Gamma_2)^2}, \quad (7)$$

which denotes the nonuniform exchange of magnons between rogue wave and background for the different spin current as shown in Fig. 4. From Eq. (7) we find the spin current can control the accumulation and dissipation rate of magnons, and there is a critical current condition, i.e., $A_{Jc} = 2k_c$. Below the critical current, the magnons exchange decreases with the increasing current term A_J . However, the magnons exchange is accelerated with the increasing current above the critical value. The roles of spin-transfer torque are completely opposite for the cases below and above the critical current which is shown in Fig. 4 (f). From Fig. 4(a) to 4(e) we see that the magnetic rogue wave can be created in the different direction for (x, t) space, which ascribes to the nonuniform exchange of magnons between rogue wave and background tuning by the spin-polarized current. When $A_J = 2k_c$, the time of magnons accumulation (or dissipation) attains its maximum. As shown the inset figure of Fig. 4 (f), i.e., the integral $\xi(x, t) = \int_{-\infty}^{+\infty} \delta(x, t) dx = 8\pi A_c / (1 + t^2 A_c^4)^{1/2}$, the magnons in background accumulate to the central part when $t < 0$. It leads to the generation of a hump with two grooves on the background along the space direction and the critical peak of the hump can occur at $t = 0$. In contrast, when $t > 0$, the magnons in the hump start to dissipate into the background so that the hump gradually decay. The magnetic rogue wave disappears ultimately, and it verifies the rogue wave is only one oscillation in temporal localization and displays a unstable dynamic behavior.

With some specific initial conditions, the excitation of rogue wave can be recovered by means of the numerical simulation. In order to understand such process of magnetic rogue wave, we choose the initial value of solution,

which can be approximated by

$$q(x, 0) = (\rho + \epsilon \chi \cos \varphi_1) \exp(i\varphi), \quad (8)$$

where $\rho = [2\kappa_1(\kappa_1 - iu_1) - A_c^2] / A_c$, $\epsilon = \exp(-x_0)$, $\chi = 4\kappa_1 u_1(\kappa_1 - iu_1) / A_c^2$ and $\varphi_1 = \kappa_1 x$ with $\kappa_1 = \sqrt{A_c^2 - u_1^2}$. By direct numerical simulations, we find that the solution of the initial value problem in Eq. (3) with initial condition Eq. (8) can be well described by the solution in Eq. (5). Fig. 5(a) is a result of direct numerical simulation, which shows that a small periodic perturbation with a very small modulation parameter can induce a near-ideal rogue wave localization, whose profile is basically consistent with the ideal theoretical limit solution of Eq. (5) as shown in Fig. 5(b). As a result, a small initial perturbation with a small modulation can induce the generation and breakup of a near-ideal rogue wave.

IV. CONCLUSIONS

In summary, we have investigated the formative mechanism of magnetic rogue wave and the properties of magnon density in uniaxial anisotropic ferromagnetic nanowire driven by spin-transfer torque. Our results show that the accumulation of energy and magnons toward to its central part plays the main role for the gen-

eration of rogue wave with stronger breathing character and rogue wave only appears at the spatial-temporal localization. We also display the rouge wave is unsuitably and gradually decay because the nonuniform exchange rate of energy and magnons which can be controlled by the spin-polarized current. A novel critical current condition is obtained analytically, and the spin-transfer torque plays the completely opposite roles for the case of below and above the critical value.

V. ACKNOWLEDGEMENT

Zai-Dong Li was supported by NSF of China under Grant No. 10874038, the Hundred Innovation Talents Supporting Project of Hebei Province of China under Grant No. CPRC014, Tianjin Municipal Natural Science Foundation of China (No. 11JCYBJC01600), and China postdoctoral science foundation under Grant No. 20100470987. This work was also supported by NSFC under grants Nos. 10874235, 10934010, 60978019, the NKBRSCF under grants Nos. 2009CB930701, 2010CB922904, 2011CB921502, 2012CB821300, and NSFC-RGC under grants Nos. 11061160490 and 1386-N-HKU748/10.

-
- [1] T. L. Gilbert, IEEE Trans. Magn. **40**, 3443 (2004).
 - [2] A. M. Kosevich, B. A. Ivanov, A. S. Kovalev, Phys. Rep. **194**, 117 (1990); H. J. Mikeska and M. Steiner, Adv. Phys. **40**, 191 (1991).
 - [3] S. S. P. Parkin, M. Hayashi, and L. Thomas, Science **320**, 190 (2008).
 - [4] A. Hubert and R. Schafer, Magnetic Domains: The Analysis of Magnetic Microstructures (Springer, New York, 2001).
 - [5] T. Ono, H. Miyajima, K. Shigeto, K. Mibu, N. Hosoi, and T. Shinjo, Science **284**, 468 (1999); D. Atkinson, D. A. Allwood, G. Xiong, M. D. Cooke, C. C. Faulkner, and R. P. Cowburn, Nat. Mater. **2**, 85 (2003).
 - [6] G. S. D. Beach, C. Nistor, C. Knutson, M. Tsoi, and J. L. Erskine, Nat. Mater. **4**, 741 (2005).
 - [7] M. Hayashi, L. Thomas, Y. B. Bazaliy, C. Rettner, R. Moriya, X. Jiang, and S. S. P. Parkin, Phys. Rev. Lett. **96**, 197207 (2006); L. Thomas, M. Hayashi, X. Jiang, R. Moriya, C. Rettner, and S. S. P. Parkin, Nature (London) **443**, 197 (2006); M. Hayashi, L. Thomas, C. Rettner, R. Moriya, Y. B. Bazaliy, and S. S. P. Parkin, Phys. Rev. Lett. **98**, 037204 (2007).
 - [8] A. Thiaville, Y. Nakatani, J. Miltat, and Y. Suzuki, Europhys. Lett. **69**, 990 (2005); S. E. Barnes and S. Maekawa, Phys. Rev. Lett. **95**, 107204 (2005); C. Heide, Phys. Rev. Lett. **87**, 197201 (2001); Kjetil Magne Dørheim Hals, A. K. Nguyen, and A. Brataas, Phys. Rev. Lett. **102**, 256601 (2009).
 - [9] J. Grollier, P. Boulenc, V. Cros, A. Hamzić, A. Vaurès, A. Fert, and G. Faini, Appl. Phys. Lett. **83**, 509 (2003).
 - [10] C. H. Marrows, Adv. Phys. **54**, 585 (2005).
 - [11] N. L. Schryer and L. R. Walker, J. Appl. Phys. **45**, 5406 (1974); M. Kläui, C. A. F. Vaz, J. A. C. Bland, W. Wernsdorfer, G. Faini, E. Cambril, L. J. Heyderman, F. Nolting, and U. Rüdiger, Phys. Rev. Lett. **94**, 106601 (2005).
 - [12] A. P. Malozemoff and J. C. Slonczewski, Magnetic Domain Walls in Bubble Material (Academic, New York, 1979).
 - [13] G. S. D. Beach, C. Knutson, C. Nistor, M. Tsoi, and J. L. Erskine, Phys. Rev. Lett. **97**, 057203 (2006); J. S. Yang, C. Nistor, G. S. D. Beach, and J. L. Erskine, Phys. Rev. B **77**, 014413 (2008).
 - [14] X. R. Wang, P. Yan, J. Lu, and C. He, Ann. Phys. **324**, 1815 (2009); X. R. Wang, P. Yan, and J. Lu, Europhys. Lett. **86**, 67001 (2009).
 - [15] J. C. Slonczewski, J. Magn. Magn. Mater. **159**, L1 (1996); L. Berger, Phys. Rev. B **54**, 9353 (1996).
 - [16] Y. B. Bazaliy, B. A. Jones, and S. C. Zhang, Phys. Rev. B **57**, R3213 (1998); J. C. Slonczewski, J. Magn. Magn. Mater. **195**, L261 (1999).
 - [17] G. Tatara and H. Kohno, Phys. Rev. Lett. **92**, 086601 (2004); J. Ho, F. C. Khanna, and B. C. Choi, Phys. Rev. Lett. **92**, 097601 (2004).
 - [18] Z. Li and S. Zhang, Phys. Rev. Lett. **92**, 207203 (2004).
 - [19] A. Yamaguchi, T. Ono, S. Nasu, K. Miyake, K. Mibu, and T. Shinjo, Phys. Rev. Lett. **92**, 077205 (2004); M. Kläui, P. -O. Jubert, R. Allenspach, A. Bischof, J. A. C. Bland, G. Faini, U. Rüdiger, C. A. F. Vaz, L. Vila, and C. Vouille, Phys. Rev. Lett. **95**, 026601 (2005).
 - [20] E. Saitoh, H. Miyajima, T. Yamaoka and G. Tatara, Na-

- ture **432**, 203 (2004).
- [21] C. K. Lim, T. Devolder, C. Chappert, J. Grollier, V. Cros, A. Vaurès, A. Fert, and G. Faini, *Appl. Phys. Lett.* **84**, 2820 (2004); G. Tatara, E. Saitoh, M. Ichimura, and H. Kohno, *Appl. Phys. Lett.* **86**, 232504 (2005).
 - [22] J. Ohe and B. Kramer, *Phys. Rev. Lett.* **96**, 027204 (2006); V. K. Dugaev, V. R. Vieira, P. D. Sacramento, J. Barnaś, M. A. N. Araújo, and J. Berakdar, *Phys. Rev. B* **74**, 054403 (2006).
 - [23] Z. D. Li, Q. Y. Li, X. R. Wang, W. M. Liu, J. Q. Liang, and Guangsheng Fu, *J. Phys.: Condens. Matter* **22**, 216001 (2010).
 - [24] *Linear and Nonlinear Spin Waves in Magnetic Films and Superlattices*, edited by M. G. Cottam World Scientific, Singapore (1994).
 - [25] M. Tsoi, A. G. M. Jansen, J. Bass, W.-C. Chiang, M. Seck, V. Tsoi, and P. Wyder, *Phys. Rev. Lett.* **80**, 4281 (1998); M. Tsoi, A. G. M. Jansen, J. Bass, W.-C. Chiang, V. Tsoi, and P. Wyder, *Nature (London)* **406**, 46 (2000).
 - [26] Y. Yamada, W. P. Van Drent, E. N. Abarra, and T. Suzuki, *J. Appl. Phys.* **83**, 6527 (1998).
 - [27] L. Belliard, J. Miltat, V. Kottler, V. Mathet, C. Chappert, and T. Valet, *J. Appl. Phys.* **81**, 5315 (1997).
 - [28] M. Tsoi, V. Tsoi, J. Bass, A. G. M. Jansen, and P. Wyder, *Phys. Rev. Lett.* **89**, 246803 (2002); J.-E. Wegrowe, X. Hoffer, Ph. Guittienne, A. Fábíán, L. Gravier, T. Wade, and J.-Ph. Ansermet, *J. Appl. Phys.* **91**, 6806 (2002).
 - [29] Z. D. Li, J. Q. Liang, L. Li, and W. M. Liu, *Phys. Rev. E* **69**, 066611 (2004); P. B. He and W. M. Liu, *Phys. Rev. B* **72**, 064410 (2005).
 - [30] Z. D. Li, Q. Y. Li, L. Li, and W. M. Liu, *Phys. Rev. E* **76**, 026605 (2007); Z. D. Li, Q. Y. Li, P. B. He, Z. G. Bai, and Y. B. Sun, *Ann. Phys. (N.Y.)* **322**, 2945 (2007).
 - [31] P. K. Shukla, I. Kourakis, B. Eliasson, M. Marklund, and L. Stenflo, *Phys. Rev. Lett.* **97**, 094501 (2006).
 - [32] B. Kibler, J. Fatome, C. Finot, G. Millot, F. Dias, G. Genty, N. Akhmediev, and J. M. Dudley, *Nat. Phys.* **6**, 790 (2010); M. Marklund and L. Stenflo, *Physics* **2**, 86 (2009); K. Hammani, B. Kibler, C. Finot, P. Morin, J. Fatome, J. M. Dudley, and G. Millot, *Opt. Lett.* **36**, 112 (2011).
 - [33] V. B. Matveev and M. ASalli, *Darboux Transformations and Solitons*, Springer Series in Nonlinear Dynamic (Springer-Verlag, Berlin, 1991).
 - [34] P. Yan, X. S. Wang, X. R. Wang, [arxiv.org/1106.4382](https://arxiv.org/abs/1106.4382).